EQUILIBRIUM STATE IN IMPACT-GENERATED POROSITY ON A LUNAR SURFACE T. Hirabayashi[1], D. A. Minton[1], H. J. Melosh[1], C. Milbury[1], Y.-H. Huang[1], and J. M. Soderblom[2], [1]Purdue University, West Lafayette, IN 47907-2051, USA, (thirabayashi@purdue.edu), [2]Massachusetts Institute of Technology, Cambridge, MA 02139, USA.

Introduction: The heavily cratered highlands of the Moon are commonly considered to have formed during the early history bombardment in the inner Solar System [1]. The lunar crater distribution provides a record for absolute-age crater chronology systems.

Recent studies have shown that cratering plays a significant role in the evolution of porosity in a surface. Impacts are capable of both increasing and decreasing crustal porosity [2], leading to an equilibrium state in impact-generated porosity [3]. Porosity also affects the cratering process, resulting in changes in the impact crater to size scaling relationships [4].

Here, we use the CTEM code [1, 5] to model the evolution of impact-generated porosity in the lunar surface. Using the results by Collins [6], we implement a new model for generating porosity in CTEM. We will then use GRAIL observations of the lunar gravity field to constrain our porosity model [2, 3].

Modeling of porous regions in CTEM: The formation of a crater starts from the contact between a projectile and a target surface, leading to strong compression. During the excavation stage, the shock wave and the following rarefaction cause the target material to be in motion, which leads to excavation flows [7]. Once slope failure occurs, the transient cavity is filled with mixed breccias and clastic debris (the final stage) [8].

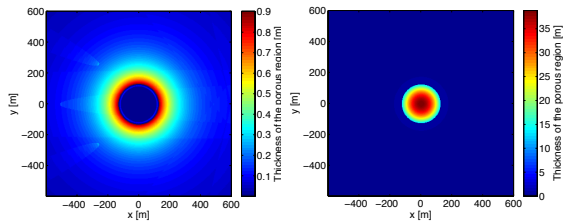

Figure 1: The thickness of the porous surface made after an impact. The impact velocity and size of the impactor are 15 km/s and 10 m, respectively. The rim diameter is 220 m. Panels a and b show the original code and the new code, respectively. The color bar of Panel a ranges from 0 to 0.9 meters, while that of Panel b does from 0 to 40 meters.

During such a process, dilatancy plays a significant role in the formation of porosity. Collins [6] reported that little dilation occurs during the excavation phase, but it becomes crucial during the final stage, leading to a dramatic change in porosity. Therefore, in CTEM, we consider material filled in the transient crater after the excavation stage to be more porous than the pre-impact target. Note that in this study, we do not analyze a detailed distribution of porosity, but consider impact-generated porosity in contrast to nonporous regions. To determine the shape of the transient crater, we compute the transient crater depth, h_t, from the rim-to-rim diameter, D_t, as $h_t = 0.3D_t$ [7]. The shape is then assumed to follow a simple parabolic profile. Because of this implementation, an impact-induced porous region obtained in the new model differs from that in the original model, which only considers excavated materials to compute the thickness of that region. In the original model, porous regolith was generated only by ejecta accumulation. In Figure 1, we contrast the old and new models. While the porosity depth is only up to 0.9 m around the rim and is zero inside the crater in the original model, it reaches up to 40 m at the center of the crater in the new model.

Also, CTEM uses a crater size scaling relationship to determine the size of an impact crater from the impactor, size, velocity, and angle [1]. The current version is capable of computing both porous and nonporous cases in the gravity regime. We show the size scaling relationship for these cases in CTEM. Figure 2 indicates the porous and nonporous scaling relationships by Wünnemann [4]. Using the form $\pi_D = C_g \pi_2^{-\beta_g}$ [4], we fix C_g and β_g at 1.34 and 0.170 for the porous cases, and at 1.32 and 0.216 for the nonporous cases, respectively (Figure 2).

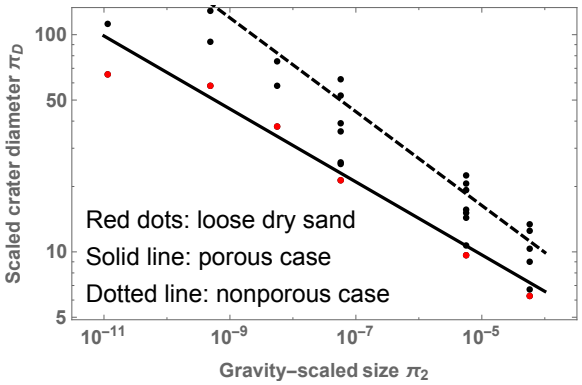

Figure 2: Crater-scaling relationships for porous and nonporous cases. The dots describe the results from iSALE simulations by Wünnemann [4], and the red dots indicate the cases of loose dry sand. In CTEM, the dotted line is implemented for the nonporous cases, while the solid line is done for the porous cases.

The scaling parameters obtained allow CTEM to control the size of a transient crater. In the code, the final crater depth is initially computed on the assumption that

the surface is nonporous. Then, if this depth is larger than the thickness of the porous layer, the program calls a routine for using the scaling law for the porosity cases.

Results: We first introduce the simulation settings. The impact velocity and size distribution profiles used are the same as used by Minton et al. [1]. We use a 720-m by 720-m square area as a test region. The side of each pixel is 3.6 meters. Initially, the surface in the test area is nonporous. To study 2 Ga evolution of a porous surface on the Moon, we conduct 200 iterations, each of which is 10 Ma. The maximum size of the crater is 720 m while the minimum size of it is 3.6 m. We do not consider the crust thickness in this study. With these settings, each case generates $\sim 1 \times 10^7$ impact craters.

Figure 3 describes the thickness of porous regions on the test area. While porous regions produced by larger impacts are obviously visible, the distribution of the thickness is quite random. The growth rate of porosity around larger craters tends to become smaller than that around smaller ones because after a large impact develops a porous region, small impacts cannot increase the porosity any further.

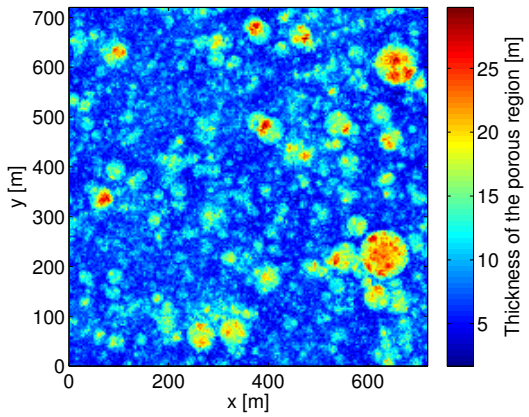

Figure 3: Thickness of the regolith layer in the test region after 2.0 Ga. The contour color ranges from 0 m to 30 m.

Figure 4 plots time-variation in the averaged thickness of the porous region over the test area. While the thickness only reaches up to 0.1 m in the original model (the red line), it increases up to 9 m in the new one (the blue line). The averaged thickness in the new model linearly increases until 1.5 Ga. However, after this period, its growth rate decreases substantially. This growth decay results from the fact that the porosity growth is in equilibrium for smaller craters, meaning that while the test area reached equilibrium for smaller impact craters, it has not yet reached equilibrium for larger impacts. The shallower slope after 1.5 Ga implies that the equilibrium point gradually shifts upward in crater diameter with time.The slopes of the porosity growth before and after 1.5 Ga are 6.4 m/Ga and 1.3 m/Ga, respectively.

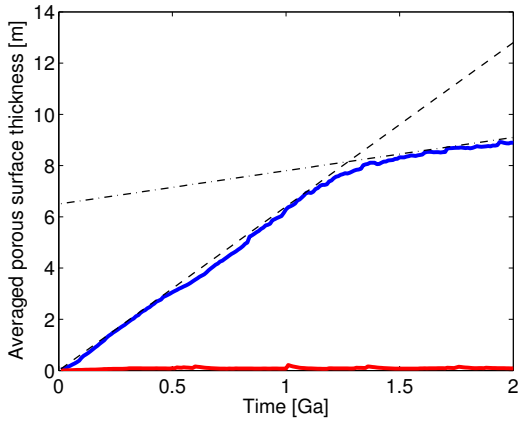

Figure 4: Variation in the average thickness of the porous surface for 2.0 Ga. This is obtained by averaging the thickness over the test area. The blue line gives the newly developed model, while the red line is for the original model. The dashed line indicates the slope for the porosity growth before 1.5 Ga, while the dot-dashed line describes that after that period. The slope is 6.4 m/Ga for the first 1.5 Ga and then decreases to 1.3 m/Ga.

The present study shows that the saturation limit of the thickness is about 9 m, consistent with earlier studies, which showed that the thickness of a regolith surface ranges from 3 m to 20 m on the Moon [9, 10]. On the other hand, if impact craters are directly responsible for the formation of porosity, the porosity layer in the lunar highland crust is no more than ~ 8 km in depth [3], consistent with estimates of the thickness of the lunar megaregolith [11]. To investigate the evolution of such a thick porous region, we will run simulations for the late heavy bombardment crater distribution. Note that as discussed by Soderblom et al. [3], the thick porous crust might have formed due to impact-generated fracturing. Further study is necessary to understand this mechanism. Also, we have not yet incorporated the detailed distribution of porosity in CTEM. As discussed by Collins [1], porosity depends on the size and impact velocity of an impactor. Implementation of this effect will be our future work.

References: [1] D. A. Minton, et al. (2015) *Icarus* 247:172. [2] C. Milbury, et al. (2015) *GRL*. [3] J. M. Soderblom, et al. (2015) *GRL* 42(17):6939. [4] K. Wünnemann, et al. (2006) *Icarus* 180(2):514. [5] J. E. Richardson (2009) *Icarus* 204(2):697. [6] G. Collins (2014) *JGR: Planets* 119(12):2600. [7] H. J. Melosh (1989) *Impact cratering: A geologic process* 1. [8] R. A. Grieve, et al. (1977) in *Impact and explosion cratering: Planetary and terrestrial implications* vol. 1 791–814. [9] V. R. Oberbeck, et al. (1968) *Icarus* 9(1):446. [10] E. Shoemaker, et al. (1969) *JGR* 74(25):6081. [11] F. Hörz, et al. (1991) *Lunar sourcebook: A users guide to the Moon* 61–120.